JGR Space Physics

RESEARCH ARTICLE
10.1029/2020JA028213

A Comparison of the Location of the Mid-Latitude Trough and Plasmapause Boundary

J. M. Weygand[1,2], I. Zhelavskaya[3,4], and Y. Shprits[1,2,3,4]

[1]Institute of Geophysics and Planetary Physics, University of California, Los Angeles, CA, USA, [2]Department of Earth, Planetary, and Space Sciences, University of California, Los Angeles, CA, USA, [3]Helmholtz Centre Potsdam, GFZ German Research Centre for Geosciences and University of Potsdam, Potsdam, Germany, [4]Institute for Physics and Astronomy, University of Potsdam Helmholtz Centre Potsdam, GFZ German Research Centre for Geosciences and University of Potsdam, Potsdam, Germany

Key Points:

- We show for a range of geomagnetic conditions that the locations of the mid-latitude trough observed in vTEC maps and IMAGE EUV measured plasmapause boundary mapped with a magnetic field line model to the ionosphere generally agree within the uncertainty
- We show that common models of the position of the plasmapause boundary mapped with a magnetic field line model to the ionosphere generally agree with the location of the mid-latitude trough

Correspondence to:
J. M. Weygand,
jweygand@igpp.ucla.edu

Citation:
Weygand, J. M., Zhelavskaya, I., & Shprits, Y. (2021). A comparison of the location of the mid-latitude trough and plasmapause boundary. *Journal of Geophysical Research: Space Physics*, *126*, e2020JA028213. https://doi.org/10.1029/2020JA028213

Received 8 MAY 2020
Accepted 16 MAR 2021

© 2021. The Authors.
This is an open access article under the terms of the Creative Commons Attribution License, which permits use, distribution and reproduction in any medium, provided the original work is properly cited.

Abstract We have compared the location of the mid-latitude trough observed in two dimensional vertical total electron content (vTEC) maps with four plasmapause boundary models, Radiation Belt Storm Probes (RBSP) observations, and IMAGE extreme ultraviolet (EUV) observations all mapped to the ionosphere pierce point using the Tsyganenko (1996) magnetic field line model. For this study, we examine four events over North America: one just after the October 13, 2012 storm, one during the April 20, 2002 double storm, another during a large substorm on January 26, 2013, and one quiet event on May 19, 2001. We have found that in general, the equatorward edge of the mid-latitude trough is within several degrees in geographic latitude of the mapped model plasmapause boundary location, the plasmapause boundary identified with IMAGE EUV, and the location identified by the RBSP spacecraft. When the mid-latitude trough is mapped to the inner magnetosphere, the observed boundary agrees with the plasmapause boundary models within two Earth Radii at nearly all local times in the nightside and the observed mid-latitude boundary is within the uncertainty of the observations at most local times in the nightside. Furthermore, during dynamic solar wind conditions of April 20, 2002, the mid-latitude trough observed in the vTEC maps propagates equatorward as the plasmapause boundary identified with IMAGE EUV moves earthward. Our results indicate that the mid-latitude trough observed within the vTEC maps represents an additional means of identifying the plasmapause boundary location, which could result in improved plasmapause boundary models.

Plain Language Summary The equatorward edge of the mid-latitude trough as observed in TEC maps indicates the location of the plasmapause boundary. We compare the location of the mid-latitude trough for four events over a range of geomagnetic conditions with plasmapause boundary identified by IMAGE extreme ultraviolet and Radiation Belt Storm Probes and the plasmapause location as indicated by four different models. We find a good agreement between some the methods even under dynamics conditions. The mid-latitude trough can supply the location for the plasmapause boundary during periods when no spacecraft are available to identify the boundary.

1. Introduction

The plasmasphere plays an important role in modulating energetic particles fluxes (e.g., Kozyra et al., 1995) and influences the propagation of ULF waves (e.g., Takahashi & Anderson, 1992; Webb & Orr, 1975a, 1975b). The plasmapause separates chorus from hiss waves, which produce acceleration and loss of particles, respectively. Radiation belt electrons inside of the plasmasphere can resonate with electromagnetic ion cyclotron waves, while outside of the plasmasphere radiation belt electrons are out of resonance. A leading mechanism for acceleration of electrons to relativistic energies includes radial diffusion driven by ULF waves, but the plasmapause is also a physical boundary that can reflect ULF waves or at least cutoff ULF waves from the plasmasphere. Therefore, understanding the dynamics of the plasmapause boundary is critical for radiation belt modeling. Furthermore, the structure of the plasmasphere is driven by the inner magnetosphere electric field and observations of the plasmasphere can help infer global electric field, which is another quantity that is difficult to directly observe. Finally, there is some coupling between the ionosphere and the plasmasphere. Shim et al. (2017) demonstrated that the coupling processes between the two regions are not simple. However, this coupling suggests that the plasmaspheric density can contribute

to the ionospheric vertical total electron content (vTEC). The vTEC observations of the mid-latitude trough are a relatively unexploited data set for studying the coupled relationship plasmapause and mid-latitude trough and provide a valuable resource for future studies and models of the plasmapause (Pedatella & Larson, 2010).

The plasmapause was first discovered in the 1960s by Carpenter (1963) using observations of whistler waves. The in situ measurements reported in Gringauz et al. (1960) using the LUNIK 2 spacecraft directly confirmed the presence of the strong density gradients. Spacecraft methods to identify the plasmapause location include using direct electron density measurements, the upper hybrid frequency to obtain the electron density (Mosier et al., 1973), and the spacecraft potential to obtain the electron density (Li et al., 2010; Pedersen et al., 2008). However, these methods can only provide single point measurements and cannot produce a global detailed picture of the asymmetric, MLT dependent plasmasphere. The IMAGE mission provided unique observations of global distribution of He+ from 2000 to 2005 that could be used as a proxy for the plasmapause and provide plasmapause boundary observations over a wide range of local times (Goldstein, 2004, 2005; Goldstein, Sandel, Forrester, & Reiff, 2003; Goldstein, Sandel, Hairston, & Reiff, 2003). While such methods provide a global picture of the MLT dependent plasmasphere they are remote line of sight observations and can certainly benefit from being validated by additional independent observations. Despite the importance of identifying the plasmapause location, regular global observations of this magnetospheric boundary are still not routinely available and plasmapause models are frequently employed to determine the location of the plasmapause boundary.

There are a number of plasmapause models in the literature. We will focus on only 4 plasmapause models here. For this study, we examine the Carpenter and Anderson (1992) empirical model, the O'Brien and Moldwin (2003) empirical model, the plasmapause test particle (PTP) simulation (Goldstein, Pascuale, et al., 2014; Goldstein, Thomsen, & DeJong, 2014), and the PINE (Plasma density in the Inner magnetosphere Neural network-based Empirical) model (Zhelavskaya et al., 2017). Carpenter and Anderson (1992) used inner magnetosphere plasma density from ISEE 1 and 2. The estimated location of the plasmapause boundary is inferred using the maximum Kp over the preceding 24 h. The shortcoming of this most widely used model is that the authors used plasmapause crossings only in the range of 00–15 h local time and no specific uncertainty in the plasmapause location is provided by the model. Plasma density estimates inferred from CRRES wave measurements were used to build the O'Brien and Moldwin (2003) plasmapause model, which can provide a plasmapause location as a function of Kp, AE, and Dst. We note that the O'Brien and Moldwin (2003) study was developed from the same data set as that of Moldwin et al. (2002). The *i* model suffers from the same challenges as Moldwin et al. (2002), including a possible bias to low Lpp on the day side due to the strict density gradient criteria used in identifying the plasmapause, and an orbital upper limit of an L shell around 7. For this study, we only use the Kp geomagnetic index and the maximum Kp over the preceding 36–2 h. O'Brien and Moldwin (2003) estimate that their RMS error is ~0.76 L in the midnight sector. We note here that the scatter plot of plasmapause location versus Kp in Figure 1 of O'Brien and Moldwin (2003) is quite similar to the scatter plot of the plasmapause location versus Kp in Carpenter and Anderson (1992) (i.e., their Figure 6). This similarity in the scatter plots suggests that the approximate uncertainty for the plasmapause location for Carpenter and Anderson (1992) is ~0.8 L and we will use this approximation in the discussion section.

The PTP simulation represents the time-varying global plasmapause as an ensemble of cold test particles subject only to *ExB* drift. The convection electric (*E*) field is scaled by the solar wind electric field and the Kp index. The PTP simulation reproduces Radiation Belt Storm Probes (RBSP) plasmapause observations to within about 0.4 L (Goldstein, Pascuale, et al., 2014; Goldstein, Thomsen, & DeJong, 2014). The PINE density model was developed using neural networks and was trained on the electron density data set from the RBSP Electric and Magnetic Field Instrument Suite and Integrated Science (EMFISIS) (Zhelavskaya et al., 2017). The model reconstructs the plasmasphere dynamics with a cross-correlation of ~0.95 on their test set and its global reconstructions of plasma density are in good agreement with the IMAGE extreme ultraviolet (EUV) images of global distribution of He+. The plasmapause is extracted from the PINE model by using electron density threshold $n_b = 10\ (6.6/L)^4\ cm^{-3}$ separating the plasmasphere from the plasma trough (Sheeley et al., 2001). We note that the PINE model results have not been examined to determine

whether the Sheeley et al. (2001) method for determining the plasmapause location routinely represents clear density gradients in the PINE model.

All the models discussed here provide smooth plasmapause boundaries as they are statistical representation and, in the case of the PTP simulations and the PINE output, they can reproduce the dayside drainage plume. However, IMAGE EUV observations of the plasmapause demonstrate that the plasmapause boundary can frequently be anything but smooth (Adrian et al., 2004; Sandel et al., 2003). On the other hand, single spacecraft in situ measurement of the plasmapause boundary will not capture all the irregularities of the plasmasphere in the same way as EUV images of plasmasphere and models based on in situ measurements may not always accurately represent plasmapause boundary.

Yizengaw et al. (2005) and Yizengaw and Moldwin (2005) have shown that the plasmapause boundary, which they identified with IMAGE EUV observations, and the equatorward edge of the mid-latitude trough, which they extracted manually, are on the same field line. Specifically, Yizengaw and Moldwin (2005) found the plasmapause boundary mapped within 1.4°–1.8° of the vTEC minimum of the mid-latitude trough. The mid-latitude trough appears as a depleted region of ionospheric electron density in the nightside F-region with sharp gradients in the electron density (i.e., vTECs) bounding the poleward and equatorward edges. It is located just equatorward of the equatorward edge of the auroral oval (Krankowski et al. 2009; Yang et al., 2015, 2016). Rodger et al. (1992) documents that the poleward edge of the mid-latitude trough is about 0.5° equatorward of the energetic electron precipitation in the evening sector. The mid-latitude trough is thought to form as a result of the stagnation of ionospheric plasma, trapped between a region of eastward (co-rotating) plasma drift, which is equatorward of the auroral oval (Whalen, 1989), and a region of westward drift in the auroral zone itself (Aladjev et al., 2001). Sub-auroral polarization streams (SAPS) and SAID are also expected to have a significant influence on the mid-latitude trough. Large potential drops imposed on the magnetotail and auroral ionosphere by solar wind driven convection E field essentially drive SAPS (Foster & Burke, 2002). Effect of SAPS on the inner magnetosphere is an intensification of the plasmapause erosion and rotation motion of duskside plasmasphere plumes (Goldstein et al., 2005; Goldstein, Sandel, Forrester, & Reiff, 2003). Within the SAPS in the ionosphere there is frictional heating which enhances the plasma temperatures. The higher plasma temperatures increase ionospheric recombination rates that leads to a deeper depletion in ionospheric electron density and conductivity (Schunk et al., 1976). Mid-latitude troughs can be identified in the vTEC data as a depletion in the vTEC values between about 45° and 60° GLat (50°–65°MLat) along latitudinal cuts of the vTECs. For the purpose of this study we define the equatorward edge of the trough as the region where the vTEC values sharply decrease from high to low values with increasing latitude between about 45° and 60° GLat but equatorward of the auroral oval. Based on this information, vTEC observations have the potential to provide limited observations of the plasmapause boundary of a wide range of longitudes over North America, Europe, and Asia.

A number of other studies have made comparisons between the vTEC mid-latitude trough and plasmapause location, using either a comparison of observations or observations against models. Anderson et al. (2008) found the locations of the mid-latitude trough observed in the DMSP H+ density are usually earthward of plasmapause locations, derived from the O'Brien and Moldwin (2003) empirical plasmapause model, on average by about 1 L shell. Furthermore, during periods when the plasmasphere and plasmapause are showing significant structure they determined in almost all of the events the DMSP derived plasmapause location is more that about 0.4 L closer to the earth than the IMAGE EUV plasmapause location. Similarly, Park et al. (2012) showed that the DMSP plasmapause location was close to the mapped IMAGE EUV plasmapause position, but provided no specific values to quantify how close. Chen et al. (2017) used electron density measurements to find the mid-latitude trough and whistler signals from ELF/VLF observations, to identify the plasmapause where both measurements were performed on the DEMETER (Detection of Electro-Magnetic Emissions Transmitted from Earthquake Regions) satellite. They found that the mid-latitude trough was about 2° poleward of the plasmapause ionospheric location (or about 0.5 L further away from the Earth in the magnetosphere) for low values of ap, but the mid-latitude trough was equatorward of the plasmapause location for more active ap conditions. The implication of the variation with ap is that the mid-latitude trough may not represent the plasmapause even though they are similarly influenced by geomagnetic activity. Lastly, Shinbori et al. (2018) compared the mid-latitude trough identified through TEC

Arase spacecraft observations with the Carpenter and Anderson (1992) model results and found the trough observations to be 1° equatorward of the model for a maximum Kp value of 4.7.

This study presents evidence that vTEC observations of the mid-latitude trough can potentially provide measurements of the plasmapause boundary and can help identify the location of the plasmasphere. In the next section, we discuss the spacecraft and instrumentation employed in this study and, in the Observations section, we examine in detail four events from, April 20, 2002, October 14, 2012, January 26, 2013, and May 19, 2001. In the Discussion we interpret the model results in relation to the mid-latitude trough observations. We also examine one dynamic case in detail.

2. Data

The data for our study comes from three sources: vTEC maps from ground-based GPS receivers, IMAGE EUV images, and electron density from the RBSP EMFISIS.

Data for vTECs values obtained from ground-based GPS receivers are available online as global vTEC maps with a cadence of 5 min through the Madrigal web server. The vTEC values are output in 1° bins of latitude and longitude. The processing of vTEC values was based on data from about 2,000 to 3,000 receivers prior to 2015. The MIT Automated Processing of GPS (MAPGPS) software suite (Rideout & Coster, 2006) estimates the vTEC values at the ionospheric pierce point at an altitude of 350 km. The MAPGPS processing code was significantly enhanced in 2015 and GPS TEC data from 2001 to 2016 were reprocessed using an updated version of MAPGPS (Vierinen et al., 2016).

The IMAGE spacecraft was launched in March of 2000. IMAGE EUV imager obtains global images of the plasmasphere by detecting 304 Å sunlight resonantly scattered by the He+ ions. Plasmapause boundary locations were extracted manually, by clicking on an EUV image with a computer mouse (Goldstein, Wolf, et al., 2004). The plasmapause boundary can consist of either a well-defined boundary or a band of scatter points. The data archive of plasmapause boundaries derived from the IMAGE EUV images are available at http://enarc.space.swri.edu/EUV/. The uncertainty associated with the plasmapause boundary location for a well-defined plasmapause is 0.3-0.7 Re.

RBSP spacecraft were launched in August 2012, and later renamed as the Van Allen Probes. The mission consists of two identical spacecraft on a near-equatorial medium earth orbit with apogee of about 4.7 Earth radii and orbital periods of about 537 min. This orbit allows the two spacecraft to make regular observations of the plasmasphere. EMFISIS makes electric field measurements in the frequency range of 10–487 kHz and magnetic field measurements in order to identify the upper hybrid resonance band, which can be used to obtain estimates of the electron density (Mosier et al., 1973). The electron density measurements can then be used to identify the plasmapause location, as the spacecraft traverses that boundary. We have used electron density measurements derived by the method described in Zhelavskaya et al. (2016). The plasmapause was identified using the density threshold n_b from Sheeley et al. (2001) separating the plasmasphere from the plasmatrough ($n_b = 10\ (6.6/L)^4\ cm^{-3}$), which agreed well with the location of a sharp drop of electron density.

3. Observations

For this study we examine four separate events on April 20, 2002, October 14, 2012, January 26, 2013, and May 19, 2001. These events were selected due to the visibility of the mid-latitude trough in the vTEC maps across most of North America. Additionally, the IMAGE EUV plasmapause boundary information (April 20, 2002 and May 19, 2001), and RBSP plasmapause boundary information is readily available, along with the PTP simulation results (October 14, 2012, and January 26, 2013).

The left panel of Figure 1 shows a two-dimensional map in geographic coordinates of the vTECs over North America and Greenland for April 20, 2002 at 0,307 UT. This event occurs during the April 18, 2002 double decrease in Dst storm index, but during this event the Dst is around −127 nT on April 18, 2002 at 07 UT and −149 nT at 08 UT on April 20, 2002, the AL index minimum is ∼−1,491 nT on April 19, 2002, and the Kp is 7.3 at 0300 UT. The geomagnetic activity for the various indices is shown in Figure 2. The color scale

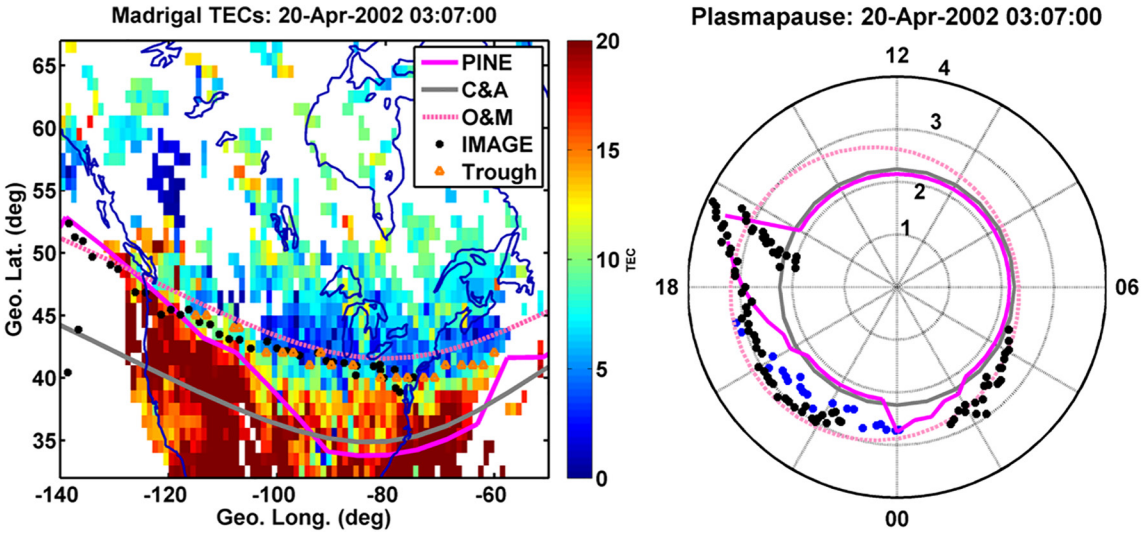

Figure 1. On the left panel is a two-dimensional vertical total electron content (vTEC) map from April 20, 2002 at 0307 UT with plasmapause boundary from three different models. The mauve curve is the PINE model and the gray curve is the Carpenter and Anderson (1992) model. The pink dotted curve is the O'Brien and Moldwin (2003) model and the black symbols are the plasmapause boundary identified with IMAGE extreme ultraviolet (EUV). The orange triangles display the equatorward edge of the mid-latitude trough. On the rightside is plasmapause boundary from the same models and the mid-latitude trough for April 20, 2002 plotted as L versus MLT. The blue symbols are the plasmapause boundary from the mapped location of the mid-latitude trough.

for the vTECs is on the right side of the plot and the range has been selected to best display the mid-latitude trough in blue, which arcs down from eastern end of the state of Washington, then down to the southern end of the Great Lakes, and up to the southern of Nova Scotia. The orange triangles display the equatorward edge of the mid-latitude trough that has been selected by eye at the sharp gradient in the vTECs. We note for this event that good vTEC observations over Europe are available. However, the mid-latitude trough in the European sector could not be clearly identified because the gradient in the vTECs most likely associated with the equatorward edge of the mid-latitude trough is at about 38° GLat and presumed equatorward edge of the mid-latitude trough is well southward of the European concentration of GPS ground stations. The presumed equatorward edge of the mid-latitude trough is located far southward of the GPS stations as a result of severe erosion of the plasmasphere into an L shell of about 2.3 as indicated by the location of the plasmapause identified using IMAGE EUV at about 4 MLT. Future studies correlating the plasmapause location and the mid-latitude trough position should account for such an extreme position of the plasmapause and the mid-latitude trough. The vTEC data shown have a 1° resolution and we have combined 40 min of data, centered on 0300 UT, to more clearly show the mid-latitude trough. For this event we have used the Tsyganenko (1996) (T96) magnetic field line model to map the plasmapause location from the inner magnetosphere for three different plasmapause models and the plasmapause location determined with IMAGE EUV down to an altitude of 350 km, which is the pierce point for the vTECs. The mauve curve shows the mapped results from the PINE model (Zhelavskaya et al., 2017) for an electron density cutoff corresponding to the density threshold n_b from Sheeley et al. (2001) separating the plasmasphere from the plasma trough ($n_b = 10\ (6.6/L)^4\ cm^{-3}$). The gray curve represents the results from the Carpenter and Anderson (1992) model where the $Kp_{24} = 7.0$, and the pink dashed curve displays the results from the O'Brien and Moldwin (2003) model where the input $Kp_{36} = 7$. The black symbols across North America, just equatorward of the O'Brien and Moldwin (2003) model, represent the plasmapause boundary identified with IMAGE EUV at 0307 UT.

The differences in the latitudinal location of the three different models and the mid-latitude trough location in Figure 1 are as large as 8° GLat across North America. From ~60° to 120° W Glong, the Carpenter and Anderson (1992) model is about 6°–8° equatorward of the mid-latitude trough within the local midnight sector. In the dusk sector from about 60° to 120° W Glong, the O'Brien and Moldwin (2003) models are within about 1°–2° of the mid-latitude trough. In the dusk sector from about 110° to 120° W Glong, the PINE model is within about 1°–3° of the mid-latitude trough. However, at 105° W Glong the PINE model is significantly further equatorward and from about 60° to 80° W Glong the PINE model boundary is equatorward

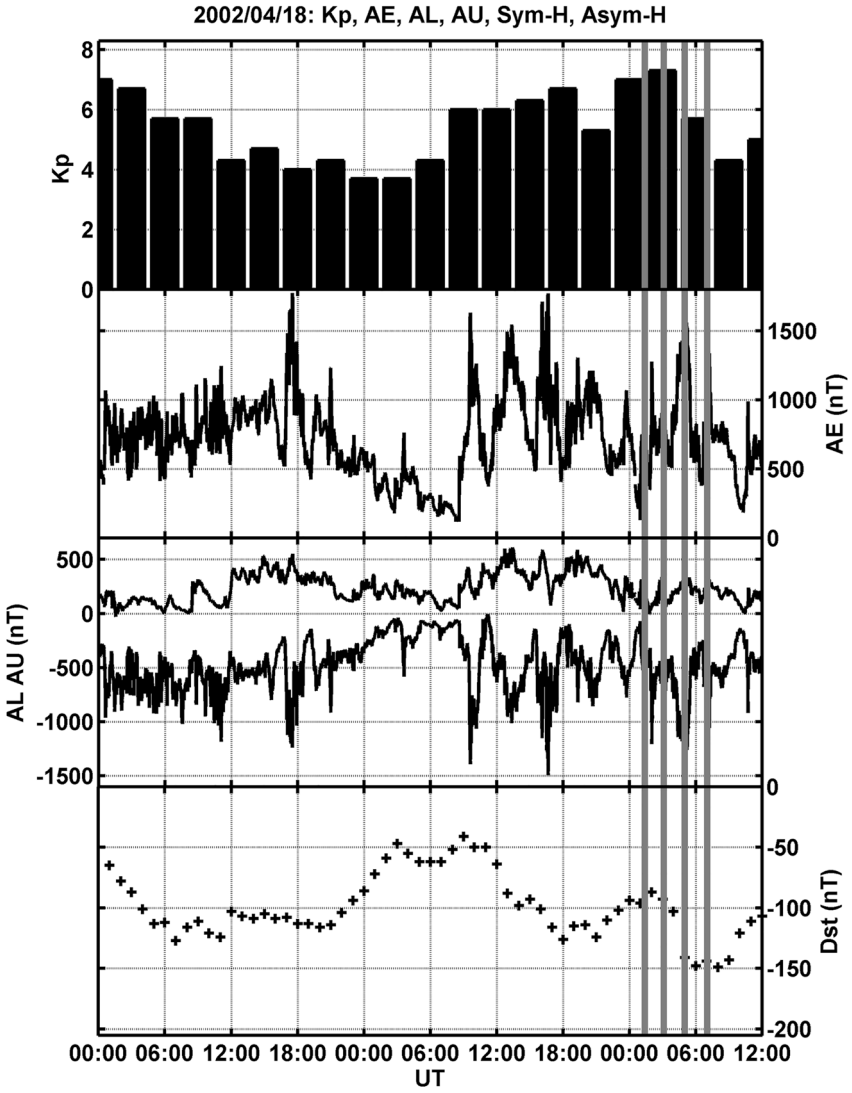

Figure 2. Geomagnetic conditions during the April 20, 2002 mid-latitude trough. The plot begins on April 18, 2002 in order to show the double storm time condition on the eighteenth and the twentieth. The top panel displays the Kp index, the second panel shows the AE index, the third panel shows the AU and AL indices, and the final panel displays the Dst index. The four vertical lines indicate various times associate with Figures 1 and 7.

of the Carpenter and Anderson (1992) model. The EUV plasmapause location closely follows the equatorward edge of the mid-latitude trough from about 75° to 120° W Glong. This similarity in locations supports the results of Yizengaw et al. (2005) and Yizengaw and Moldwin (2005) who show that the plasmapause boundary and the equatorward edge of the mid-latitude trough are approximately collocated.

Another method of comparing the plasmapause boundaries and the location of the mid-latitude trough is to plot the plasmapause boundary and magnetic field line mapped mid-latitude trough as L versus MLT. In other words, the mid-latitude trough location can be used to estimate the plasmapause location. The right panel of Figure 1 shows the different plasmapause boundary model locations, the T96 magnetic field line mapped equatorward boundary of the mid-latitude trough, and the IMAGE EUV plasmapause boundary as a function of L versus MLT plot, to demonstrate the differences in the radial location for the April 20, 2002 event. Magnetic local noon is at the top side of the plot, magnetic midnight is at the bottom, dawn on the right, and dusk on the left of the figure. The blue symbols are the mid-latitude trough mapped from the ionosphere at an altitude of 350 km (the vTEC pierce point) to approximately the largest radial distance using the T96 model, with the appropriate solar wind propagated to the bow shock and geomagnetic index

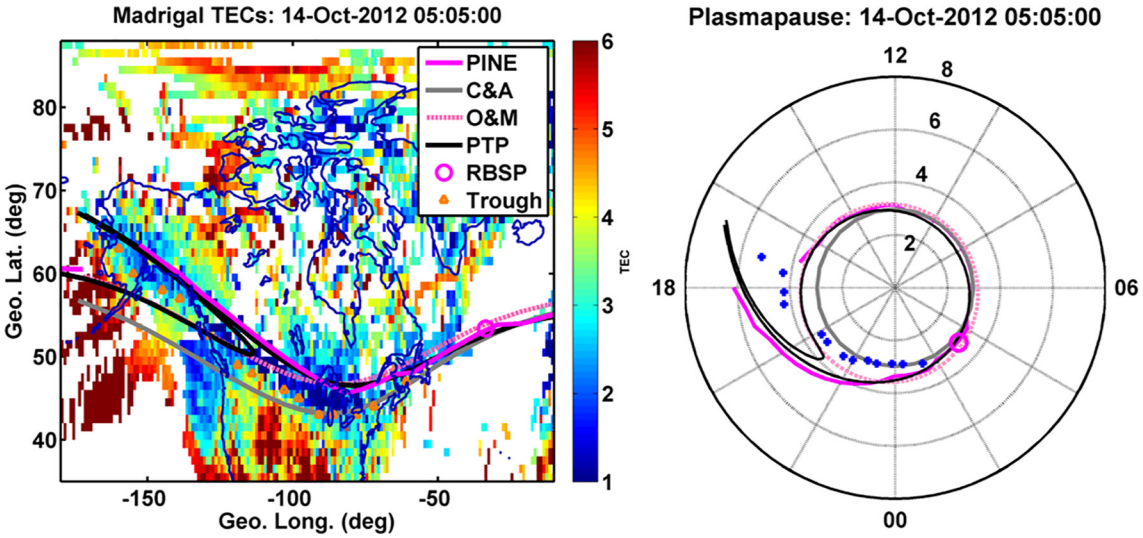

Figure 3. On the leftside is a two dimensional vertical total electron content (vTEC) map from October 14, 2012 with plasmapause boundary from four different models. This figure has the same format as Figure 1. The black curve is the PTP simulation results and the mauve "o" symbol in the Atlantic is the plasmapause boundary identified with RBSP-B. On the rightside is the plasmapause boundary from various models and the mid-latitude trough for October 14, 2012. The black curve is the PTP simulation results. The blue symbols are the plasmapause boundary from the mapped location of the mid-latitude trough and the mauve "o" is the plasmapause boundary identified with RBSP-B. RBSP, Radiation Belt Storm Probes.

inputs. The mid-latitude trough was selected from the vTEC maps manually, visible as the lower edge of the blue band in the vTEC maps (i.e., *where there is a sharp gradient in the vTEC values*), except in the region of about 130 W GLong where the trough could not be clearly identified. The method of manually selecting the equatorward edge of the mid-latitude trough is similar to the method used by Goldstein et al. (2004) for selecting the plasmapause boundary within the IMAGE EUV images.

The right panel of Figure 1 shows a number of results. First, the differences between the models in the pre-midnight sector are as large as about 1 Re for the PINE model and Carpenter and Anderson (1992) model, which has an estimated uncertainty of about 0.8 Re. Second, the mapped location of the mid-latitude trough appears to agree generally with the O'Brien and Moldwin (2003) model, within the uncertainty of 0.76 Re in the midnight sector. From ~19 to 22.5 MLT, the IMAGE EUV plasmapause location and the mapped mid-latitude trough location generally agree within the uncertainty of IMAGE EUV observations, which are on the order of 0.3–0.7 Re. The agreement between the mapped mid-latitude trough location and the IMAGE EUV identified plasmapause boundary demonstrates that the equatorward edge of the mid-latitude trough and the plasmapause boundary are collocated within about ±2°. Finally, the PINE model predicts the drainage plume in the dusk sector at about the same MLT location and the same radial distance as the IMAGE EUV observations of a drainage plume.

The left panel of Figure 3 shows the two-dimensional map in geographic coordinates of the vTECs over North America and Greenland, for October 14, 2012 at 0505 UT. The format for this figure is the same as Figure 1**.** This event occurs about 22 h after the October 13, 2012 storm, however during this event the Dst is about −36 nT for the hour just before the event, the AL index is about −100 nT, and the Kp at the time of this event is 3. The color scale has been selected to best display the mid-latitude trough in blue, which extends from central Alaska down to the Great Lakes area and then back up to Gulf of St Lawrence. We have combined 40 min of vTEC data centered on 0505 UT to clearly show the mid-latitude trough. We note that for this event, extensive vTEC observations over Europe and South America are available, however, we could not clearly identify a mid-latitude trough. Using the Tsyganenko (1996) (T96) model, we have mapped this event for the plasmapause location, from the inner magnetosphere for four different models and the plasmapause location determined with RBSP, down to the ionosphere at 350 km. The mauve curves show the mapped results from the PINE model (Zhelavskaya et al., 2017), the gray curve represents the results from the Carpenter and Anderson (1992) model where the $Kp_{24} = 5.7$, the pink curves displays the results from the O'Brien and Moldwin (2003) where the input $Kp_{36} = 5.7$, and the black curves shows

the approximate location of the PTP simulation (Goldstein, Pascuale, et al., 2014; Goldstein, Thomsen, & DeJong, 2014). In Figure 3, we have used the PTP simulation plasmapause location derived for the October 14, 2012 at 0500 UT. The mauve "o" symbol over the Atlantic is the plasmapause boundary identified with RBSP-B at 0436:50 UT.

The differences in the latitudinal location of the four different models and the mid-latitude trough location in Figure 3 are as large as 6° GLat across North America. No model clearly follows the equatorward edge of the vTEC mid-latitude trough, but some models do closely map to part of the trough. From ∼60° to 100° W GLong the Carpenter and Anderson (1992) model follows the equatorward edge of the trough within about 2° GLat in the local midnight sector. In the dusk sector from about 130° to 170° W GLong around Alaska the PINE and O'Brien and Moldwin (2003) models are within about 3° of the equatorward edge of the mid-latitude trough. The PTP simulation shows part of the plasmaspheric plume from about 110° to 180° W GLong. This plume is not visible within the vTECs observations, most likely due to the spatial resolution of the vTEC data. Around 80° W GLong the PTP simulation is poleward of the mid-latitude trough boundary by about 1°–3° and in the west side of North America the PTP model is about 1°–3° equatorward of the location of the mid-latitude trough.

The right panel of Figure 3 shows the different plasmapause boundary model locations, the T96 magnetic field line mapped equatorward boundary of the mid-latitude trough, and the RBSP plasmapause boundary as a function of L versus MLT plot, to demonstrate the differences in the radial location for the October 14, 2012 event. The format of this figure is the same as Figure 1. The black curve is the PTP simulation results, and the blue symbols are the mid-latitude trough mapped from the ionosphere to the magnetic equator. The mauve "o" at about 04 MLT marks the RBSP-B location measured at 0436:50 UT.

The important features in Figure 3 model and data comparison are: first, the differences between the models in the midnight sector are generally within 1 Re for the Carpenter and Anderson and O'Brien and Moldwin model. Second, the mapped location of the mid-latitude trough appears to agree generally within the uncertainty of the Carpenter and Anderson (1992) model location (∼0.8 Re) and the O'Brien and Moldwin (2003) model. The mapped location is not always within the uncertainty, for the most part of the PTP simulation, which is 0.4 Re, especially at the location of the plasmaspheric plume. The PINE model, similar to the PTP simulation, predicts the drainage plume in the dusk sector, which is not observed in the vTECs at the mapped location of the mid-latitude trough.

The left panel of Figure 4 displays the two dimensional map of the vTECs over North America and Greenland for January 26, 2013 at 0930 UT. The format for this figure is the same as Figure 1. We have combined 40 min of vTEC data centered on 0930 UT to more clearly show the mid-latitude trough. We note for this event that extensive vTEC observations over Europe and South America are available, but we could not clearly identify a mid-latitude trough. Prior to this event the Dst is about −22 nT for the hour before the event, the Kp is 3.3, the AL index is about −700 nT just after a substorm onset that began about 0835 UT. During this event the foot points of the two RBSP spacecraft are located over North America on the western side of the continent. The mauve triangle and "o" symbol over Western Canada represent the plasmapause boundary identified with RBSP-A at 09:10:46 UT and B at 09:53:50 UT, respectively. We again used a plasma density cutoff n_b from Sheeley et al. (2001) for the PINE model (Zhelavskaya et al., 2017) to identify the plasmapause location. The $Kp_{24} = 4.3$ for the Carpenter and Anderson (1992) model and $Kp_{36} = 4.3$ for the O'Brien and Moldwin (2003). Finally, in Figure 4 we have shown the PTP simulation plasmapause location derived for the January 26, 2013 at 0930 UT.

During this event the differences between the latitudinal location of the four different models and the mid-latitude trough location, as can be seen on Figure 4, are about 3° GLat across North America. No model clearly follows the equatorward edge of the vTEC mid-latitude trough, but some models closely map to within a few degrees to part of the trough. From ∼130° to 55° W GLong the PTP model follows the equatorward edge of the mid-latitude trough within about 1°–2° of latitude and the Carpenter and Anderson (1992) model follows the equatorward edge of the trough within about 2°–3° GLat in the local midnight sector. At all longitudes the PINE and the O'Brien and Moldwin models are further poleward by ∼2° of the equatorward edge of the mid-latitude trough. We also note that even the RBSP plasmapause locations map to higher latitudes then the mid-latitude trough.

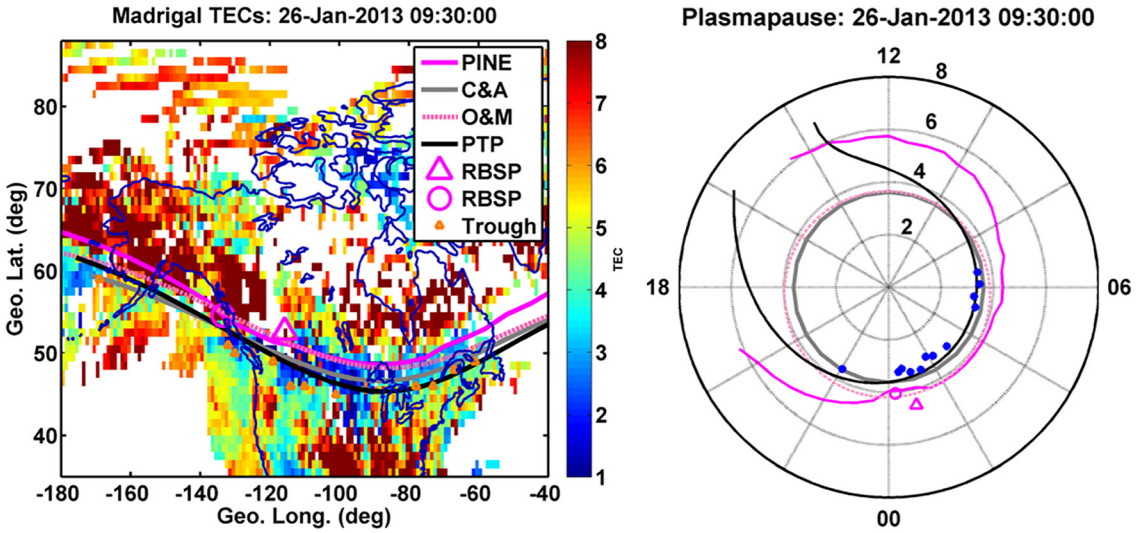

Figure 4. On the leftside is a two dimensional vertical total electron content (vTEC) map from January 26, 2013 with plasmapause boundary from four different models. This figure has the same format as Figure 1. The mauve triangle and "o" symbols over western North America indicate the plasmapause boundary identified with RBSP-A and B, respectively. On the rightside is the plasmapause boundary for the same models and the mid-latitude trough for January 26, 2013. The mauve triangle and "o" symbols mark the plasmapause boundary location identified by RBSP-A and B, respectively. RBSP, Radiation Belt Storm Probes.

The right panel of Figure 4 shows the plasmapause location for the January 26, 2013 event. This figure has the same format as Figure 3. The mauve triangle and "o" symbols are the RBSP-A and B identifications of the plasmapause boundary, respectively. The model plasmapause boundaries differ by more than 2 Re in some places, especially in the dusk sector and dayside. In the midnight sector, the mid-latitude trough plasmapause boundary is within about 0.5 Re of the Carpenter and Anderson model and the PTP simulation except at ∼5 MLT and ∼22 MLT. At about 00 MLT the PINE model and O'Brien and Moldwin model are also close to the mid-latitude trough plasmapause boundary. The PINE model is within about 0.8 Re in the 22-00 MLT sector but is radially further out in the 02–06 MLT sectors. Similarly, the O'Brien and Moldwin model is further radially in the region of 4 MLT. The PTP model predicts a wide plasmaspheric plume in the dusk sector, but none of the other models clearly show a plasmaspheric plume and no plume is clearly visible in the mapped vTEC data.

In the last three events, we examined moderate to active geomagnetic conditions. The left panel of Figure 5 shows the two dimensional map of the vTECs over North America and Greenland for May 19, 2001 at 0808 UT. The format for this figure is the same as Figure 1**.** We have combined 40 min of vTEC data centered on 0808 UT to more clearly show the mid-latitude trough. We note for this event that good vTEC observations over Europe are available, but again it was not possible to clearly identify the mid-latitude trough. Prior to this event the average Dst is about −16 nT for the 8 h before the event, the Kp decreases from 4 to 1, the AL index is about −100 nT after a substorm onset that ended at about 0520 UT. During this event the plasmapause boundary determined using IMAGE EUV is available from about 60° to 120° W Glong and is denoted with black symbols. The EUV plasmapause location follows the equatorward edge of the mid-latitude trough from about 75° to 120° W Glong. However, equatorward edge of the mid-latitude trough in the vTEC observations is not smooth and differs from the EUV plasmapause location by 2°–5° in some places. We again used a plasma density cutoff n_b from Sheeley et al. (2001) for the PINE model (Zhelavskaya et al., 2017) to identify the plasmapause location. The Kp = 4 for both the Carpenter and Anderson (1992) model and for the O'Brien and Moldwin (2003) model.

The right panel of Figure 5 shows the plasmapause location for the May 19, 2001 event. The IMAGE EUV plasmapause boundaries and Carpenter and Anderson model differ by about 1 Re in between about 23 and 24 MLT. In the post-midnight sector, the mid-latitude trough plasmapause boundary is within about 0.5 Re of the IMAGE EUV plasmapause boundary and Carpenter and Anderson model. The PINE model lies at

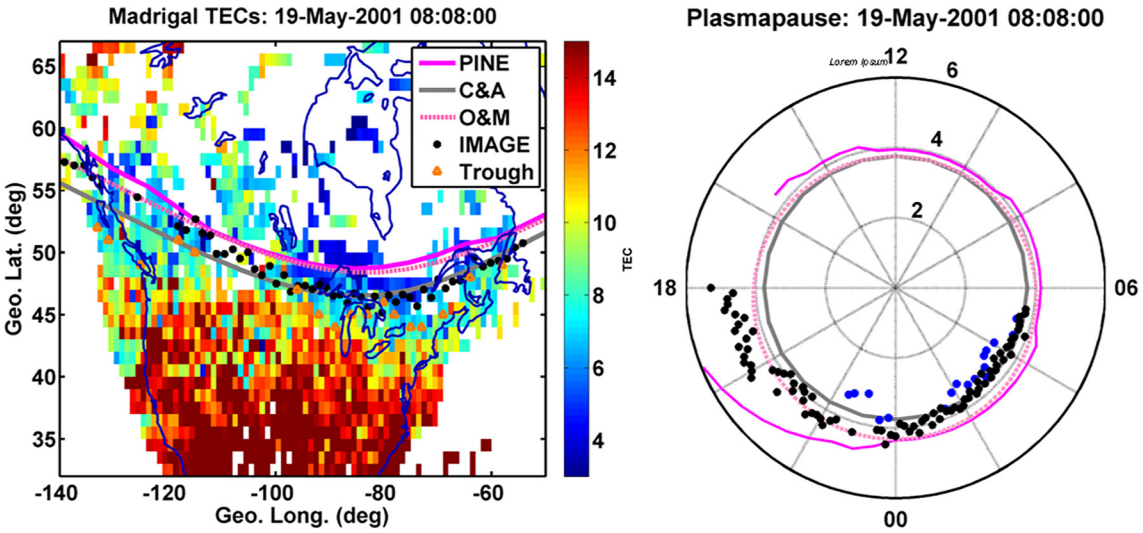

Figure 5. On the leftside is a two dimensional vertical total electron content (vTEC) map from May 19, 2001 with plasmapause boundary from three different models. This figure has the same format as Figure 1. On the rightside is the plasmapause boundary for the same models and the mid-latitude trough for May 19, 2001.

a larger radius than the mid-latitude trough plasmapause and differs by about 1 Re or more. Similarly, the O'Brien and Moldwin model is further radially than the mid-latitude trough plasmapause.

4. Discussion and Conclusions

Figures 1 and 3–5 demonstrate that the results from the plasmapause models are similar to each other and generally follow the mid-latitude trough, but upon closer inspection there are noticeable differences. The Carpenter and Anderson (1992) model follows the equatorward edge of the mid-latitude trough within 1°–3° of latitude at ~80° W GLong for October 14, 2012 event and the full local time coverage of the January 26, 2013 event. The Carpenter and Anderson (1992) model was about ~2°–4° poleward of the mid-latitude trough in the May 19, 2001 event, but about ~4°–6° equatorward at the dusk ~150° W GLong for the October 14, 2012 event and 4°–6° equatorward in the April 20, 2002 event. The O'Brien and Moldwin (2003) model follows the mid-latitude trough for the April 20, 2002 event, but it is always about 1°–3° poleward of the mid-latitude trough. Furthermore, the O'Brien and Moldwin (2003) model is poleward of the mid-latitude trough by about 2°–5° for the October 14, 2012, January 26, 2013, and May 19, 2001 events. The PINE model is consistently about 2°–5° poleward of the mid-latitude trough for October 14, 2012, the January 26, 2013, and May 19, 2001 events. During the April 20, 2002 event, the mid-latitude trough is between 2° and 7° equatorward of the mid-latitude trough. Lastly, the PTP model is 0°–3° poleward of the mid-latitude trough for the January 26, 2013, but it is poleward of the mid-latitude trough at local midnight by 2°–5° for the October 14, 2012 and equatorward of the mid-latitude trough by 2°–5° in the local dusk.

Our observations are similar to previous studies. Specifically, Yizengaw and Moldwin (2005) found the IMAGE EUV plasmapause boundary mapped to 1.4°–1.8° of the vTEC minimum of the mid-latitude trough, whereas we found the IMAGE EUV plasmapause boundary mapped to within 3° of the equatorward edge of the mid-latitude trough. Anderson et al. (2008) found that the mid-latitude trough identified by DMSP was typically about 0.4 L closer to the Earth than the IMAGE EUV observations. We also found that the equatorward edge of the vTEC mid-latitude trough is typically closer to the Earth than seen in the IMAGE EUV observations. Our results are in contrast to Park et al. (2012) who determined that the DMSP identified mid-latitude trough was close to the location of the IMAGE EUV plasmapause. Our results are also significantly different from Chen et al. (2017) which compared the mid-latitude trough location with the plasmapause location using electron density and whistler signals from ELF/VLF observations from the DEMETER spacecraft. They found the trough was poleward of the plasmapause location for quiet *ap* conditions, but the mid-latitude trough was equatorward of the plasmapause location for active *ap* conditions. The most similar

comparison to our study was given in Shinbouri et al. (2018) which compared the mid-latitude trough in the Arase spacecraft TEC observations with the Carpenter and Anderson (1992) model. They found the trough to be 1° poleward for moderately active conditions. For the most active geomagnetic conditions we found the Carpenter and Anderson results to be 4°–6° equatorward. For the quieter geomagnetic conditions the Carpenter and Anderson (1992) results are 0°–3° poleward of the vTEC mid-latitude trough. The Carpenter and Anderson (1992) model follows the mid-latitude trough within a 0°–3° of latitude, both poleward and equatorward for the October 14, 2012 and the January 26, 2013 events, which were of moderate Kp activity.

All of the four events presented are from the North American region. This bias toward North America raises the question of the global validity of the findings. The North American sector is a specific region, due to the tilt and offset of the magnetic dipole. Unfortunately, the mid-latitude trough was not observed over other regions during the events considered in this study. Our results should be considered specific to that sector and future studies should investigate other regions such as Europe and Asia.

All of the models discussed have some uncertainty associated with the plasmapause location, in addition to uncertainties associated with the mapped mid-latitude trough plasmapause location in the T96 field line mapping, and the uncertainty in manually selecting the equatorward edge of the mid-latitude trough. The uncertainty associated with the T96 model is challenging to determine. As far as we are aware there is only one study that examines in detail the uncertainty associated with mapping for the T96 model (Pulkkinen & Tsyganenko, 1996). To obtain the uncertainty we determined the Kp value for each event and estimated the uncertainty from various figures in Pulkkinen and Tsyganenko (1996), based on the mid-latitude trough location from our events. If we use Pulkkinen and Tsyganenko (1996) as a guide, then for a Kp of about 3 for both the October 14, 2012, and January 26, 2013 events, the uncertainty at the lowest latitude is in the order of 0–0.2 Re. If we treat the uncertainty in selecting the equatorward edge of the mid-latitude trough as 1°–2° in latitude and calculate the differences in L-shell location with the T96 mapping, then the uncertainty is in the order of 0.2–0.4 Re. The largest mid-latitude trough uncertainty (~0.4 Re) then overlaps with many of the other plasmapause model boundaries for the January 26, 2013 substorm event and the October 14, 2012 event. However, there is still a significant difference between the mid-latitude trough plasmapause boundary and most of the models in the April 20, 2002 event and the May 19, 2001 quiet event. These significant differences for both the extremely active and quiet periods suggest that the models examined work well during moderate geomagnetic conditions, but not as well during quiet to extreme conditions. The models may not follow the mid-latitude trough as closely for extremely active periods because there are poor statistics on these events and more observations are required to improve the models for extremely active conditions. Furthermore, the models may not closely represent the mid-latitude trough during quiet periods because the mid-latitude trough is difficult to clearly identify in quiet conditions, when the plasmasphere is inflated and images of the plasmasphere are diffused. However, we are encouraged to note that the mid-latitude trough uncertainty overlaps with the IMAGE EUV plasmapause boundary location for the April 20, 2002 storm event and for most of the May 19, 2001 quiet event. Finally, the January 26, 2013 substorm is the only event with RBSP plasmapause observations at about the same MLT location as the mapped mid-latitude trough. Both RBSP measurements are over 0.8 Re away from the mapped mid-latitude trough location and closest to the PINE model plasmapause. This proximity is to be expected, since this model relies on RBSP observations. This difference could be due to improperly selecting the location of the mid-latitude trough, or the RBSP values for the plasmapause location may not be ideal.

We compared the mid-latitude trough and plasmapause boundary models for a range of geomagnetic activity for a number of specific instances, but how well do the plasmapause boundary models perform during dynamic conditions? Figure 6 displays the solar wind plasma, interplanetary magnetic field and solar wind electric field during the April 2002 double decrease in storm starting on April 19, 2002 at 1200 UT and ending on April 20, 2002 at 1200 UT. We remind the reader that Figure 2 provides the geomagnetic conditions during this period. The top three panels of Figure 6 show the interplanetary magnetic field. The *By* component at the start of the twentieth flips from about −20 nT at about 0200 UT–~18 nT by about 0400 UT. The *Bz* component early on the twentieth reaches 16 nT, sharply decreases to ~−20 nT before 0100 UT, and then remains below 0 nT for the next 6 h. The *Vx* (fourth panel) component of the solar wind is less than −550 km/s and the density (fifth panel) spikes several times between 5 and 20 #/cm^3 from about 2130 UT on the nineteenth to about 0700 UT on the twentieth. This series of jumps in the density translates to a

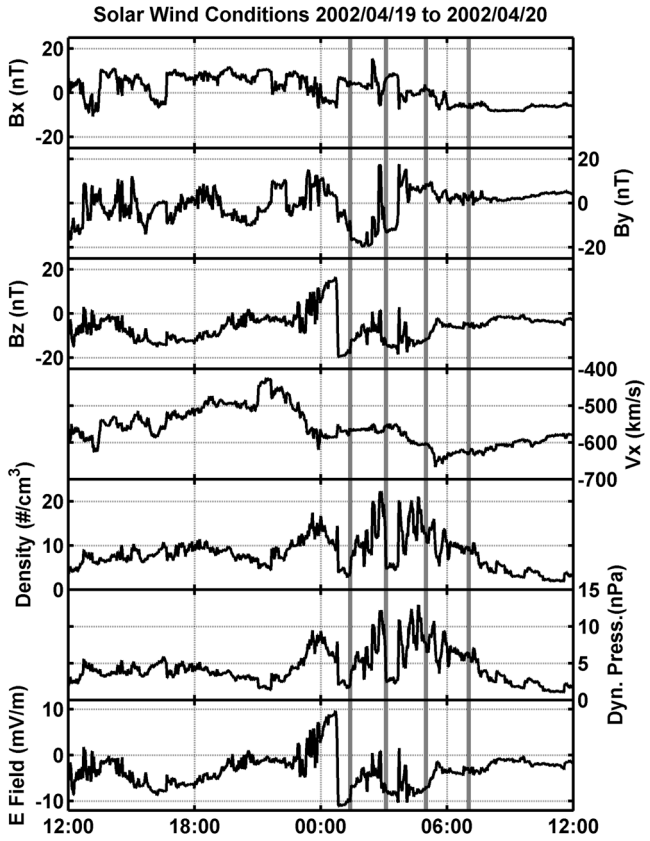

Figure 6. Solar wind conditions for April 19 and 20, 2002. The top three panels show the solar wind interplanetary magnetic field. The fourth and fifth panels display the solar wind Vx component and the number density. The bottom two panels display the dynamic pressure and the solar wind y component of the electric field. The four gray vertical lines demark the four times shown in Figures 1 and 7.

series of spikes in the solar wind dynamic pressure (sixth panel), over the same period. In the bottom panel, we have used the *Vx* and the *Bz* components to derive the *y* component of the solar wind electric field. At about 0045 UT the *Ey* peaks at about 9 mV/m and then sharply drops to just under −10 mV/m. Then electric field, in general, increases to about −1 mV/m by 0800 UT. These solar wind conditions demonstrate how significantly the solar wind dynamic pressure and electric field vary between 0125 and 0707 UT. Figure 7, along with Figure 1, show the gradual equatorward motion of the mid-latitude trough (vTEC maps in the top row) and variation of the plasmapause boundary for both the IMAGE EUV observations and the various plasmapause models (bottom row). The IMAGE EUV observations suggest that the plasmapause boundary moves from about 3 Re to about 2 Re between 0125 and 0707 UT. Similarly, the mapped magnetic field line location of the mid-latitude trough indicates that the plasmapause boundary migrates from just under 3 Re to about 2 Re. This inward motion of the plasmapause boundary as determined from the mid-latitude trough is similar to the inward motion of the plasmapause observed with IMAGE EUV, which Goldstein et al. 2004, 2005 attributed to plasmapause erosion due an increase in the solar wind electric field. However, the mid-latitude trough is just as well correlated with the interplanetary magnetic field *Bz* component, which suggests that magnetopause compression may play a role (Goldstein, Sandel, Forrester, & Reiff, 2003). Fortunately, DMSP F14 and F15 ion drift meter data are available between 0100 and 0700 UT and indicate that SAPS are present throughout this period. Both DMSP F14 and F15 (data not shown). DMSP F14 at about 0119, 0302, 0444, and 0629 UT is within the vicinity of 19 MLT and DMSP F15 at about 0238, 0420, and 0603 UT is near about 20 MLT. Both spacecraft measured sunward flow exceeding 1 km/s equatorward of the auroral oval precipitation, suggesting that SAPS are present and that the plasmapause has been eroded due to the solar wind electric field. For the vTEC trough and IMAGE EUV observations at 0125, 0307, 0410, and 0601 UT the peak SAPS speeds are within the mid-latitude trough and about 3.5°–6° poleward of the equatorward edge of the mid-latitude trough in the vTECs and about 1°–5° poleward of the IMAGE EUV plasmapause ionospheric location.

In the bottom row of Figure 7 (and the right side of Figure 2) the O'Brien and Moldwin (2003) model (dashed pink circle) and the Carpenter and Anderson (1992) model (gray circle) do not change significantly in the radial and MLT directions over the time period shown in Figure 7. These models do not change significantly because they vary as a function of the max Kp in the prior 24 h (Carpenter & Anderson, 1992) or 36 h (O'Brien & Moldwin, 2003) and not a function of the solar wind electric field. On the other hand, the PINE model is driven by the 48-h time history of the geomagnetic conditions given by averages over previous 3, 6, 9, 12, 24, 36, and 48 h of AE, Kp, SYM-H indices and also the F10.7 index. The plasmapause boundary determined by the PINE model moves radially inward more than the other two models, and agrees well with the IMAGE EUV plasmapause on the dawn sector. The differences with the mid-latitude trough plasmapause boundary are large, however, at other local times, particularly in the dusk sector. These discrepancies between the PINE model and observations may be the result of the criteria by which the plasmapause was determined in this study (i.e., using the density threshold from Sheeley et al. (2001)). More work is needed to verify whether the plasmapause location determined using these criteria routinely represents clear density gradients in PINE. We also note that the April 20, 2002 event is an active storm (Dst of −149 nT) and the models discussed in Figures 2 and 7 are all empirical models that are statistical in nature and cannot be expected to represent the plasmapause boundary at any given time.

It has been shown that the evolution of the electric field in the solar wind has a direct control over the processes in the magnetosphere such as convection, injection of particles, and plasmapause erosion. The solar

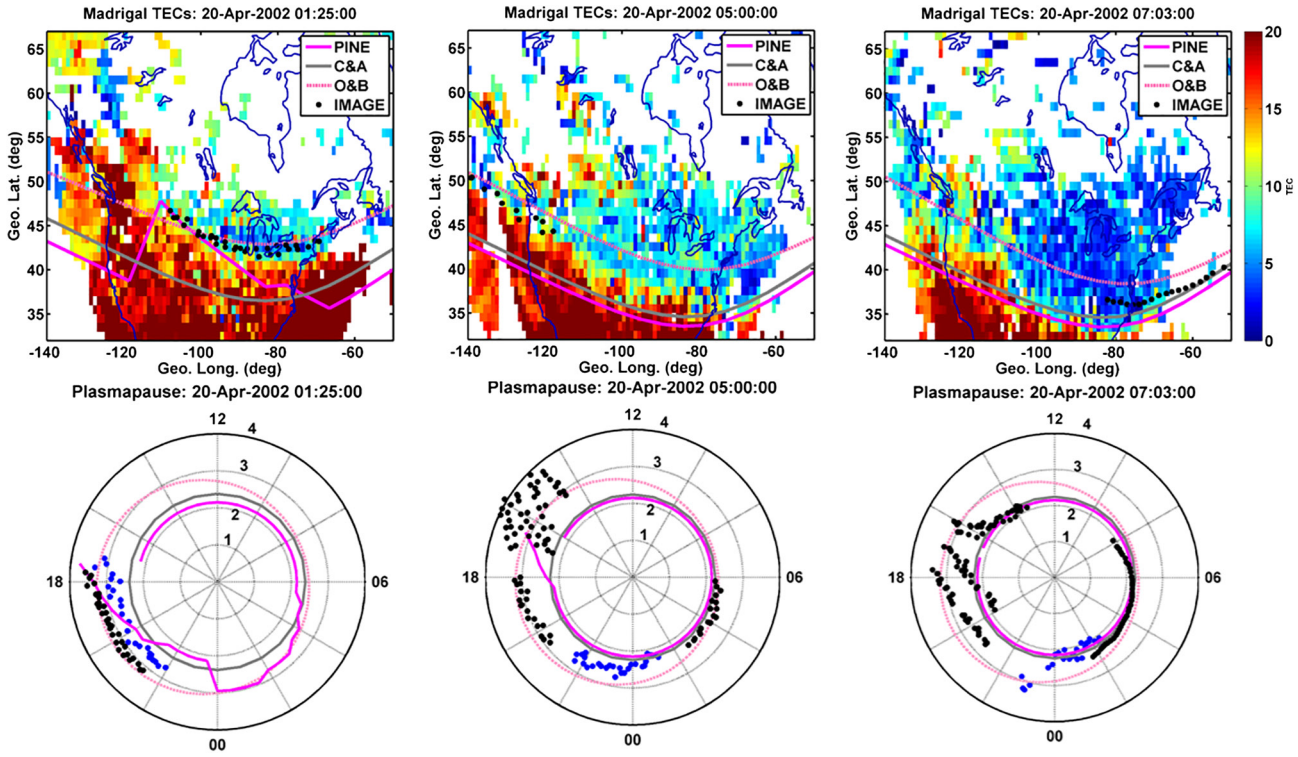

Figure 7. Three different vertical total electron content (vTEC) maps of the mid-latitude trough (top row) and plasmapause boundaries (bottom row) for 0125, 0500, and 0703 UT. These plots have a format similar to Figure 1.

wind electric field has indirect control over scattering by controlling the location of the plasma density and plasma waves that are critical for scattering particles into the atmosphere, and in turn controls ionospheric parameters such as vTEC. Such interconnection of various spatial regions and physical quantities allow the space physics community to utilize these nonliner correlations for future machine learning based empirical models of the magnetospheric and ionospheric quantities, which then can be used for predictions of magnetospheric and ionospheric quantities. Another approach of estimating these physical quantities, which are not directly observed, is parameter estimation in data assimilation. When global physical models of the environment are available, the unobserved quantities such as the mid-latitude trough or the plasmapause boundary, can be determined through known cross-correlations (e.g., Kondrashov et al., 2007).

The vTEC data represent a potential new source of data to derive the plasmapause location, which is apparent in Figures 1, 3–5, and 7. These data are limited to regions with good GPS receiver coverage, which typically occurs over land, and the mid-latitude trough is not always visible within the vTEC maps. However, two dimensional vTEC maps at Madrigal are available from 1998 to present and can add to the overall data set of plasmapause locations for periods when in situ plasmapause observations were not available and during periods of extreme active geomagnetic conditions. Finally, as we have shown here, these vTEC mid-latitude trough observations can provide constraints on present plasmapause models, but a larger statistical study should be performed.

Data Availability Statement

The authors thank Dr. J. Goldstein for maintaining the data archive of plasmapause boundaries, which are available at http://enarc.space.swri.edu/EUV/, and for maintaining the data archive of Plasmapause Test Particle (PTP) simulations, which are available at http://enarc.space.swri.edu/PTP/.

Acknowledgments
The authors acknowledge NASA THEMIS contract NAS5-02099 and NASA HPDE contract 80GSFC17C0018 at UCLA. This study was made possible by NASA HiDEE award numbers NNX16AD63G and NNX14AJ77G. I. Zhelavskaya was supported by Geo.X, the Research Network for Geosciences in Berlin and Potsdam, under Grant No SO_087_GeoX. This project has received funding from the European Union's Horizon 2020 research and innovation programme under grant agreement No. 870452 (PAGER). This research is also supported by the Helmholtz Pilot Projects Information and Data Science II, Machine learning based plasma density model project (MAP) - ZT-I-0022. We thank the members of the MIT Haystack Observatory for maintaining the Madrigal Database, which is available at: http://cedar.openmadrigal.org/. The authors would also like to thank Dr. K.-H. Glassmeier, Dr. M.G. Kivelson, Dr. R.J. Strangeway, Dr. A. Coster, and Dr. R.J. Walker for their invaluable input.

References

Adrian, M. L., Gallager, D. L., & Avanov, L. A. (2004). IMAGE EUV observation of radially bifurcated plasmaspheric features: First observations of a possible standing ULF waveform in the inner magnetosphere. *Journal of Geophysical Research*, *109*, A01203. https://doi.org/10.1029/2003JA009974

Aladjev, G. A., Evstafiev, O. V., Mingalev, V. S., Mingaleva, G. I., Tereshchenko, E. D., & Khudukon, B. Z. (2001). Interpretation of ionospheric F-region structures in the vicinity of ionisation troughs observed by satellite radio tomography. *Annales Geophysicae*, *19*, 25. https://doi.org/10.5194/angeo-19-25-2001

Anderson, P. C., Johnston, W. R., & Goldstein, J. (2008). Observations of the ionospheric projection of the plasmapause. *Geophysical Research Letters*, *35*, L15110. https://doi.org/10.1029/2008GL033978

Carpenter, D. L. (1963). Whistler evidence of a 'knee' in the magnetospheric ionization density profile. *Journal of Geophysical Research*, *68*(6), 1675–1682. https://doi.org/10.1029/jz068i006p01675

Carpenter, D. L., & Anderson, R. R. (1992). An ISEE/whistler model of equatorial electron density in the magnetosphere. *Journal of Geophysical Research*, *97*, 1097–1108. https://doi.org/10.1029/91ja01548

Chen, C. Y., Liu, T. J., Lee, I. T., Rothkaehl, H., Przepiorka, D., Chang, L. C., et al. (2017). The midlatitude trough and the plasmapause in the nighttime ionosphere simultaneously observed by DEMETER during 2006–2009. *Journal of Geophysical Research: Space Physics*, *123*, 5917–5932. https://doi.org/10.1029/2017JA024840

Foster, J. C., & Burke, W. J. (2002). SAPS: A new categorization for sub-auroral electric fields. *Eos, Transactions American Geophysical Union*, *83*(36), 393–394. https://doi.org/10.1029/2002EO000289

Goldstein, J., Pascuale, S. D., Kletzing, C., Kurth, W., Genestreti, K. J., Skoug, R. M., et al. (2014). Simulation of Van Allen probes plasmapause encounters. *Journal of Geophysical Research: Space Physics*, *119*, 7464–7484. https://doi.org/10.1002/2014JA020252

Goldstein, J., Sandel, B. R., Forrester, W. T., & Reiff, P. H. (2003). IMF-driven plasmasphere erosion of 10 July 2000. *Geophysical Research Letters*, *30*(3), 1146. https://doi.org/10.1029/2002GL016478

Goldstein, J., Sandel, B. R., Forrester, W. T., Thomsen, M. F., & Hairston, M. R. (2005). Global plasmasphere evolution 22-23 April 2001. *Journal of Geophysical Research*, *110*, A12218. https://doi.org/10.1029/2005JA011282

Goldstein, J., Sandel, B. R., Hairston, M. R., & Reiff, P. H. (2003). Control of plasmaspheric dynamics by both convection and sub-auroral polarization stream. *Geophysical Research Letters*, *30*(24), 2243. https://doi.org/10.1029/2003GL018390

Goldstein, J., Thomsen, M. F., & DeJong, A. (2014). In situ signatures of residual plasmaspheric plumes: Observations and simulation. *Journal of Geophysical Research: Space Physics*, *119*, 4706–4722. https://doi.org/10.1002/2014JA019953

Goldstein, J., Wolf, R. S., Sandel, B. R., & Reiff, P. H. (2004). Electric fields deduced from plasmapause motion in IMAGE EUV images. *Geophysical Research Letters*, *31*, L01801. https://doi.org/10.1029/2003gl018797

Gringauz, K. I., Bezrokikh, V. V., Ozerov, V. D., & Rybchinskii, R. E. (1960). A study of the interplanetary ionized gas, high-energy electrons and corpuscular radiation from the sun by means of the three-electrode trap for charged particles on the second soviet cosmic rocket. *Soviet Physics - Doklady*, *5*, 361–364.

Kondrashov, D., Shprits, Y., Ghil, M., & Thorne, R. (2007). A Kalman filter technique to estimate relativistic electron lifetimes in the outer radiation belt. *Journal of Geophysical Research*, *112*, A10227. https://doi.org/10.1029/2007JA012583

Kozyra, J. U., Rasmussen, C. E., Miller, R. H., & Villalon, E. (1995). Interaction of ring current and radiation belt protons with ducted plasmaspheric hiss: 2. Time evolution of the distribution function. *Journal of Geophysical Research*, *100*, 21911–21919. https://doi.org/10.1029/95ja01556

Krankowski, A., Shagimuratov, I. I., Ephishovo, I. I., Krypiak-Gregorczyk, A., & Yakimova, G. (2009). The occurrence of the mid-latitude ionospheric trough in GPS-TEC measurements. *Advances in Space Research*, *43*(11), 1721–1731. https://doi.org/10.1016/j.asr.2008.05.014

Li, W., Thorne, R. M., Bortnik, J., Nishimura, Y., Angelopoulos, V., Chen, L., et al. (2010). Global distributions of suprathermal electrons observed on THEMIS and potential mechanisms for access into the plasmasphere. *Journal of Geophysical Research*, *115*, A00J10. https://doi.org/10.1029/2010JA015687

Moldwin, M. B., Downward, L., Rassoul, H. K., Amin, R., & Anderson, R. R. (2002). A new model of the location of the plasmapause: CRRES results. *Journal of Geophysical Research: Space Physics*, *107*, SMP-2 10.1029/2001JA009211

Mosier, S. R., Kaiser, M. L., & Brown, L. W. (1973). Observations of noise bands associated with the upper hybrid resonance by the Imp 6 radio astronomy experiment. *Journal of Geophysical Research*, *78*, 1673–1679. https://doi.org/10.1029/ja078i010p01673

O'Brien, T. P., & Moldwin, M. B. (2003). Empirical plasmapause models from magnetic indices. *Geophysical Research Letters*, *30*(4), 1152. https://doi.org/10.1029/2002GL016007

Park, S., Kim, K.-H., Kil, H., Jee, G., Lee, D.-H., & Goldstein, J. (2012). The source of the steep plasma density gradient in middle latitudes during the 11-12 April 2001 storm. *Journal of Geophysical Research*, *117*, A05313. https://doi.org/10.1029/2011JA017349

Pedatella, N. M., & Larson, K. M. (2010). Routine determination of the plasmapause based on COSMIC GPS total electron content observations of the midlatitude trough. *Journal of Geophysical Research*, *115*, A09301. https://doi.org/10.1029/2010JA015265

Pedersen, A., Lybekk, B., André, M., Eriksson, A., Masson, A., Mozer, F. S., et al. (2008). Electron density estimations derived from spacecraft potential measurements on Cluster in tenuous plasma regions. *Journal of Geophysical Research*, *113*, A07S33. https://doi.org/10.1029/2007JA012636

Pulkkinen, T. I., & Tsyganenko, N. A. (1996). Testing the accuracy of magnetospheric model field line mapping. *Journal of Geophysical Research*, *101*(A12), 27431–27442. https://doi.org/10.1029/96ja02489

Rideout, W., & Coster, A. (2006). Automated GPS processing for global total electron content data. *GPS Solutions*, *10*(3), 219–228. https://doi.org/10.1007/s10291-006-0029-5

Rodger, A. S., Moffett, R. J., & Quegan, S. (1992). The role of ion drift in the formation of ionization troughs in the mid- and high-latitude ionosphere- A review. *Journal of Atmospheric and Terrestrial Physics*, *54*(1), 1–30. https://doi.org/10.1016/0021-9169(92)90082-v

Sandel, B. R., Goldstein, J., Gallagher, D. L., & Spasojevic, M. (2003). Extreme ultraviolet imager observations of the structure and dynamics of the plasmasphere. In *Magnetospheric imaging—The image prime mission* (pp. 25–46). Dordrecht. Springer.

Schunk, R. W., Banks, P. M., & Raitt, W. J. (1976). Effects of electric fields and other processes upon the nighttime high-latitude Flayer. *Journal of Geophysical Research*, *81*, 3271–3282. https://doi.org/10.1029/JA081i019p03271

Sheeley, B. W., Moldwin, M. B., Rassoul, H. K., & Anderson, R. R. (2001). An empirical plasmasphere and trough density model: CRRES observations. *Journal of Geophysical Research*, *106*(A11), 25631–25641. https://doi.org/10.1029/2000ja000286

Shim, J. S., Jee, G., & Scherliess, L. (2017). Climatology of plasmaspheric total electron content obtained from Jason 1 satellite. *Journal of Geophysical Research: Space Physics*, *122*, 1611–1623. https://doi.org/10.1002/2016JA023444

Shinbori, A., Otsuka, Y., Tsugawa, T., Nishioka, M., Kumamoto, A., Tsuchiya, F., et al. (2018). Temporal and spatial variations of storm time midlatitude ionospheric trough based on global GNSS-TEC and Arase satellite observations. *Geophysical Research Letters*, *45*, 7362–7370. https://doi.org/10.1029/2018GL078723

Takahashi, K., & Anderson, B. J. (1992). Distribution of ULF energy (f < 80 mHz) in the inner magnetosphere: A statistical analysis of AMPTE CCE magnetic field data. *Journal of Geophysical Research*, *97*(10), 751. https://doi.org/10.1029/92ja00328

Tsyganenko, N. A. (1996). *Effects of the solar wind conditions on the global magnetospheric configuration as deduced from data-based field models*. European Space Agency Publication.

Vierinen, J., Coster, A. J., Rideout, W. C., Erickson, P. J., & Norberg, J. (2016). Statistical framework for estimating GNSS bias. *Atmospheric Measurement Techniques*, *9*, 1303–1312. https://doi.org/10.5194/amt-9-1303-2016

Webb, D., & Orr, D. (1975a). Spectral studies of geomagnetic pulsations with periods between 20 and 120 sec, and their relationship to the plasmapause region. *Planetary and Space Science*, *23*, 1551–1561. https://doi.org/10.1016/0032-0633(75)90007-0

Webb, D., & Orr, D. (1975b). Statistical studies of geomagnetic pulsations with periods between 10 and 70 sec and their relationship to the plasmapause region. *Planetary and Space Science*, *23*, 1169–1178. https://doi.org/10.1016/0032-0633(75)90166-X

Whalen, J. A. (1989). The daytime F layer trough and its relation to ionospheric-magnetospheric convection. *Journal of Geophysical Research*, *94*(17), 17169–17184. https://doi.org/10.1029/ja094ia12p17169

Yang, N., Le, H., & Liu, L. (2015). Statistical analysis of ionospheric mid-latitude trough over the Northern Hemisphere derived from GPS total electron content data. *Earth, Planets and Space*, *67*(1), 196. https://doi.org/10.1186/s40623-015-0365-1

Yang, N., Le, H., & Liu, L. (2016). Statistical analysis of the mid-latitude trough position during different categories of magnetic storms and different storm intensities. *Earth, Planets and Space*, *68*(1), 171. https://doi.org/10.1186/s40623-016-0554-6

Yizengaw, E., & Moldwin, M. B. (2005). The altitude extension of the mid-latitude trough and its correlation with plasmapause position. *Geophysical Research Letters*, *32*, L09105. https://doi.org/10.1029/2005gl022854

Yizengaw, E., Wei, H., Moldwin, M. B., Galvan, D., Mandrake, L., Mannucci, A., & Pi, X. (2005). The correlation between mid-latitude trough and the plasmapause. *Geophysical Research Letters*, *32*, L10102. https://doi.org/10.1029/2005GL022954

Zhelavskaya, I. S., Shprits, Y. Y., & Spasojevic, M. (2017). Empirical modeling of the plasmasphere dynamics using neural networks. *Journal of Geophysical Research: Space Physics*, *122*(11), 11227–11244. https://doi.org/10.1002/2017ja024406

Zhelavskaya, I. S., Spasojevic, M., Shprits, Y. Y., & Kurth, W. S. (2016). Automated determination of electron density from electric field measurements on the Van Allen Probes spacecraft. *Journal of Geophysical Research: Space Physics*, *121*(5), 4611–4625. https://doi.org/10.1002/2015ja022132